

BEAM-BEAM EFFECTS AND DYNAMIC β^*

W. Herr (CERN, Geneva, Switzerland)

Abstract

The implications of strong beam-beam effects on luminosity measurements are discussed and estimated.

BEAM-BEAM EFFECTS IN THE LHC RELEVANT FOR VAN DER MEER SCANS

Colliding beams provide a strong electromagnetic force on the opposing beam and in the case of strong beams like the LHC, one must expect significant effects. Important effects relevant for the determination of luminosity are:

- Orbit effects caused by beam-beam kick (during scan less than 1 μm)
- Optics changes due to (de-)focusing force
- Effects change during a luminosity scan: not constant (LEP: β_y^* changed by a factor 2 !)

Since the optics changes under the influence of the beam-beam force, this has to be taken into account calculating the beam-beam force itself. Therefore it is required to compute all the effects self-consistently [1, 2, 3]. In the general case of several interaction points, this is most conveniently done using a general purpose optics program which can handle non-linear beam-beam elements. The CERN code MAD-X can be used for that purpose and all LHC optics are available in the necessary format.

Beam-beam force

An example of the shape of the beam-beam force is shown in Fig. 1, where the beam-beam force (kick) is shown as a function of the amplitude. While for small amplitudes the force is rather linear and resembles a quadrupolar field, for larger amplitudes the force becomes very non-linear. This has consequences for the luminosity scan (Van der Meer scan) since the beam-beam effects can change during such a scan. Furthermore, since the focusing strength is related to the derivative of the force with respect to the amplitude (i.e. local slope of the force), the focusing (or de-focusing) changes sign during a scan for separation larger than $\approx 1.6 \sigma$ (see e.g. Fig. 1). This is a phenomenon well known for long range beam-beam interactions [1].

Beam-beam induced β -beating

Since the linear part of the beam-beam force is similar to a quadrupolar field, one must expect an additional focusing or defocusing effect from the beam-beam interaction. Assuming a distortion (interaction point) at a position s ,

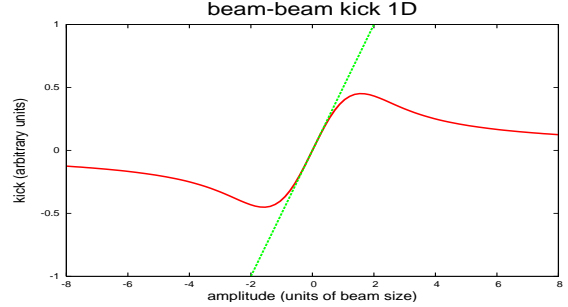


Figure 1: Beam-beam force (red line) as function of amplitude for round beams [1]. Green line corresponds to linear force of a quadrupole.

the change of the β -function at another position s_0 can be computed using:

$$\Delta\beta(s_0) = -\frac{\beta(s_0)}{2\sin(2\pi Q)} \int_{s_0}^{s_0+C} I(s) ds \quad (1)$$

with the integrand $I(s)$:

$$I(s) = \beta(s)\Delta k(s)\cos[2(\mu(s) - \mu(s_0)) - 2\pi Q] \quad (2)$$

Here C is the circumference, $k(s)$ the gradient produced by the beam-beam interaction, Q the tune of the machine and $\mu(s)$ the phase at position s . In the cases we are interested in, both, s and s_0 are interaction points. To find the distortion at the interaction point s_0 , the integral has to be taken over all other interaction points present.

DYNAMIC β - SINGLE INTERACTION POINT

A particularly interesting case is where $s = s_0$, i.e. the distortion at the interaction point where the beam-beam interaction takes place. In this case the integral can be simplified and written as [1]:

$$\frac{\beta^*}{\beta_0^*} = \frac{1}{\sqrt{1 + 4\pi\xi\cot(2\pi Q) - 4\pi^2\xi^2}} \quad (3)$$

The main parameters are the beam-beam strength ξ and the tune Q of the machine, both can strongly influence the result.

Implementation

To study the dynamic β effect self-consistently, the general purpose optics code MAD-X was used. It allows to install beam-beam elements at interaction points which are

taken into account to compute the optical functions. A Van der Meer scan is simulated by changing a bump across the beam-beam interaction point. Only the effect of head-on collisions are taken into account in this study. The result of this computation are the distorted optical functions and the change of the tunes.

Dynamic β - static case

The behaviour of the relative β change as a function of the tune Q and for different values of the beam-beam strength ξ is shown in Fig. 2. For larger beam-beam

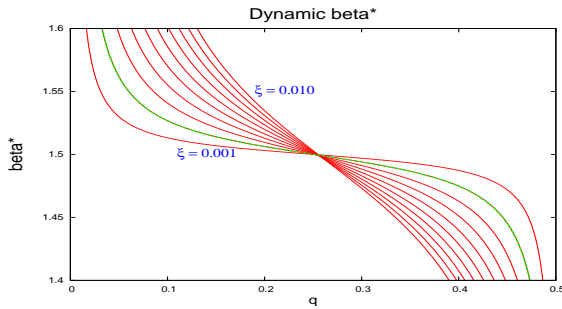


Figure 2: Dynamic β as function of tune and beam-beam strength ξ . [1]. Green line indicates typical value for beam-beam strength parameter ξ .

strengths the effect is stronger and for tune values close to the integer or half integer the change diverges. In the literature this effect is usually called "dynamic β ". Before the case of a luminosity scan is considered, the static conditions with purely head-on collisions are treated. The Tab. 1

Collisions	IP1		IP5	
	β_x^*	β_y^*	β_x^*	β_y^*
no	1.500	1.500	1.500	1.500
IP1	1.491	1.489	1.484	1.527
IP5	1.484	1.527	1.491	1.489
IP1 + IP5	1.475	1.516	1.475	1.516

Table 1: Dynamic β^* (absolute value) for one or two interactions points, $\beta_0^* = 1.5$ m.

summarizes the expected β functions at IPs 1 and 5 in the case of no, one or two collision points.

The parameters used in this case correspond to the usual conditions during luminosity scans, i.e. bunch intensity $0.85 \cdot 10^{11}$ p/bunch, a normalized emittance of $4 \mu\text{m}$, energy of 3.5 TeV and in this case an unperturbed β of 1.5 m. The Tab. 2 shows the same results except the relative changes are given.

DYNAMIC β - MULTIPLE INTERACTION POINTS

The situation is more complicated in the case of more than one interaction point and an optics code is necessary

Collisions	IP1		IP5	
	β_x^*/β_{0x}^*	β_y^*/β_{0y}^*	β_x^*/β_{0x}^*	β_y^*/β_{0y}^*
no	1.000	1.000	1.000	1.000
IP1	0.994	0.993	0.989	1.018
IP5	0.989	1.018	0.994	0.993
IP1 + IP5	0.983	1.011	0.983	1.011

Table 2: Dynamic β^* (relative change) for one or two interactions points, $\beta_0^* = 1.5$ m.

for the evaluation. For a special study, the beams were partially separated in all other IPs but the one where the scan was performed. Two cases are considered, horizontal as well as vertical separation. These cases are shown in tables Tabs. 3 and 4. Given are the head-on dynamic β for one single head-on collision and a (constant) separation of 1.4σ in all other interaction points. Because of the additional

Collisions	β_x^*	β_y^*	β_x^*/β_{0x}^*	β_y^*/β_{0y}^*
IP2	9.9427	10.1427	0.9943	1.0143
IP5	1.4922	1.5221	0.9948	1.0147
IP8	2.9974	3.0510	0.9991	1.0170

Table 3: Dynamic β^* (absolute and relative change) for head-on collision in single IP, horizontal separation of 1.4σ in all other IPs.

Collisions	β_x^*	β_y^*	β_x^*/β_{0x}^*	β_y^*/β_{0y}^*
IP2	9.9711	9.9635	0.9971	0.9964
IP5	1.5003	1.4947	1.0002	0.9965
IP8	3.0723	2.9905	1.0241	0.9968

Table 4: Dynamic β^* (absolute and relative change) for head-on collision in single IP, vertical separation of 1.4σ in all other IPs.

focusing or defocusing effects of the separated beams, the resulting changes are slightly larger.

Dynamic β - evolution during transverse scan

The most interesting question is what happens to the optical functions during a transverse scan, i.e. when the beam-beam force changes like shown in Fig. 2. The results of a horizontal and vertical scan on the β -functions are shown in Fig. 3. In the plane where the scan is performed one can clearly see the effect of the changing beam-beam force, in particular since the focusing strength (derivative of force with respect to amplitude) changes the sign. The changes during a scan are of the same order as the change by the head-on collision.

As a cross check, the horizontal and vertical tune shifts ($\Delta Q_x, \Delta Q_y$) have been computed during the scan and for

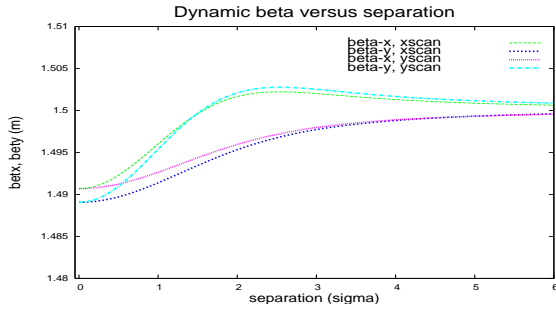


Figure 3: Dynamic β^* in IP1 during a horizontal and vertical Van der Meer scan. Collisions in IP1 only.

the horizontal scan they are shown in Fig. 4 as a function of the horizontal separation. The changes follow exactly the

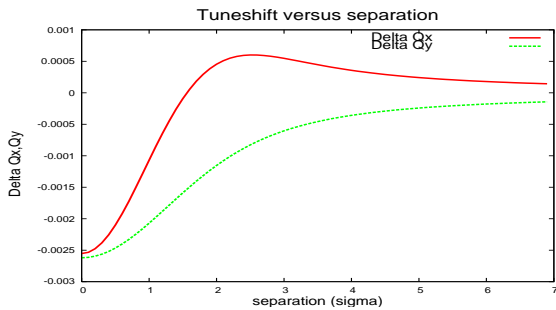


Figure 4: Beam-beam tune shifts ($\Delta Q_x, \Delta Q_y$) during a horizontal Van der Meer scan. Collisions in IP1 only.

expected behaviour.

MULTIPLE INTERACTION POINTS - SCAN

Cases with different number of head-on collisions are shown in Figs. 5 to 8. Different collision points and number of collision points are studied. It is clear that the

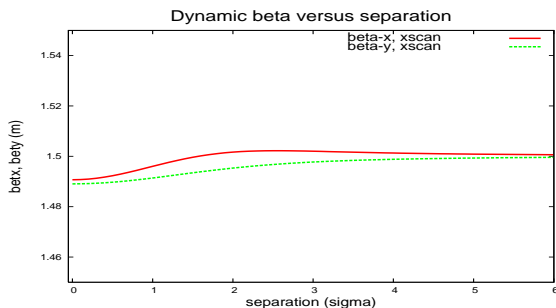


Figure 5: Dynamic β^* in IP1 during a horizontal scan. No other collisions.

shape of the β -change during a scan does not depend on additional collision points, however the starting point of the scan strongly depends on the integrated focusing from all other IPs. The behaviour during horizontal and vertical scans in IP1 with separated collisions (1.4σ in scanning

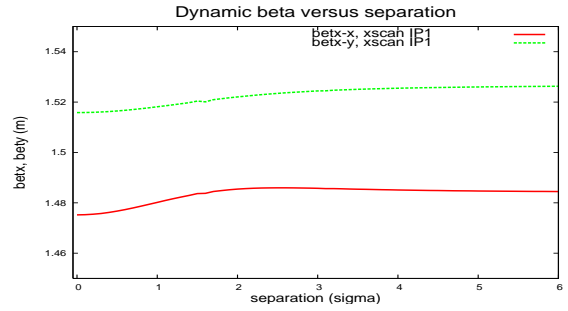


Figure 6: Dynamic β^* in IP1 during a horizontal scan. Head-on collision in IP5.

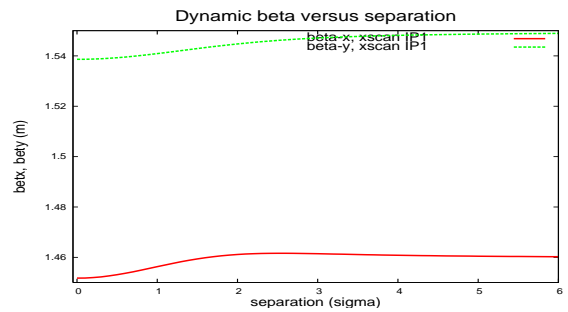


Figure 7: Dynamic β^* in IP1 during a horizontal scan. Head-on collisions in IP2 and IP5.

plane) in the other interaction points is shown in Fig. 9, confirming the observations above.

To show this standard behaviour during a scan, in Fig. 10 the horizontal β^* is shown during horizontal scans in IP1 for different, additional collision points. They correspond to the scans shown in Figs. 5 - 8. For this comparison, the starting values of β^* have been shifted for plotting purpose to the nominal value. A similar plot is shown in Fig. 11, showing the vertical β^* during a vertical scan in IP2, i.e. with a nominal β^* of 10 m. This scan was done at a different energy (1.38 TeV) and a slightly larger beam-beam strength. This demonstrates the regular shape during a scan, provided the β^* is shown as a function of the separation in units of σ and for the same strength of the beam-beam parameter ξ . This could be used to simplify the correction of systematic errors during the scan by using

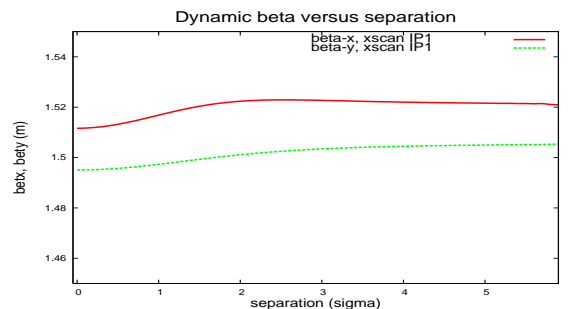


Figure 8: Dynamic β^* in IP1 during a horizontal scan. Head-on collision in IP8.

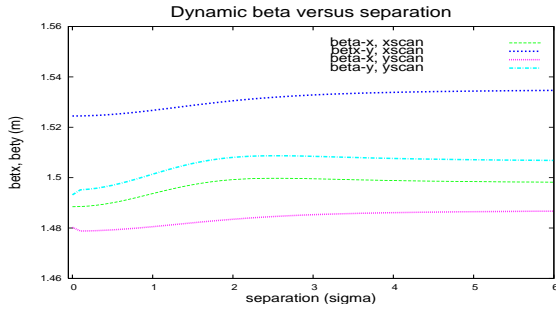


Figure 9: Dynamic β^* in IP1 during horizontal and vertical scans. Separated collisions (1.4σ in scanning plane) in all other interaction points.

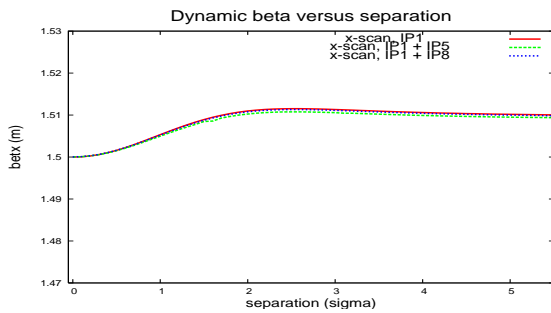


Figure 10: Dynamic β^* in IP1 during a horizontal scan for 3 collision patterns. Shifted to unperturbed β^* .

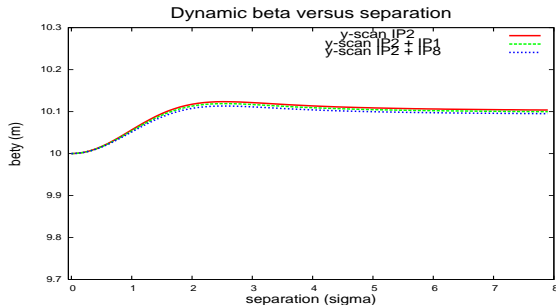


Figure 11: Dynamic β^* in IP2 during a vertical scan for 3 collision patterns. Shifted to unperturbed β^* .

the shape. The table in the Appendix A shows the change of horizontal and vertical β^* as a function of the beam separation in σ during a horizontal scan. In the case of a vertical scan the values of β_x and β_y should be swapped. A scaling for different beam-beam parameters may have to be applied using N/ϵ_n , where N is the number of particles per bunch and ϵ_n the normalized emittance. The table in the appendix has been produced with $N = 1.0 \cdot 10^{11}$ p/bunch and $\epsilon_n = 4.0 \mu\text{m}$. The table is available in computer readable format at [4].

EFFECT OF PHASE ADVANCE ERRORS

Since the integrated focusing and therefore the change of β around the machine depends on the phase advance, one may speculate whether imperfections leading to phase

advance errors can significantly change the results.

When the β -beating is corrected for physics conditions to values typically of the order of 10%, the remaining phase advance can be estimated and as an example for the phase change between interaction points 1 and 5, we get $\Delta\mu_{15} \approx (0.017 \pm 0.011) \cdot 2\pi$ [5]. Simulating such a phase error with MAD, the additional change of the beating from beam-beam is of the order 0.3%, i.e. significantly smaller than the values computed for head-on and separated collisions.

SUMMARY

To summarize the optical effects from the beam-beam interaction:

- For LHC beams the dynamic β effects are visible and of order 1%.
- For more than one head-on collision, the can become significant.
- The behaviour changes during a luminosity scan in a predictable form which is not sensitive to additional collision point.
- The dynamic β strongly depends on the number of collisions and the collision scheme.

ACKNOWLEDGEMENTS

These studies have been triggered by discussions with W. Kozanecki and his input to the calculations have been vital.

REFERENCES

- [1] W. Herr, "Beam-beam effects", CERN Accelerator School, Zeuthen 2003, in: CERN 2006-002 (2006).
- [2] W. Herr and H. Grote, "Self-consistent orbits with beam-beam effects in the LHC", Proc. 2001 Workshop on beam-beam effects, FNAL, 25.6.-27.6.2001, (2001).
- [3] W. Herr, "Features and implications of different LHC crossing schemes", CERN LHC Project Report 628 (2003).
- [4] Tables are available in computer readable format at: <http://cern.ch/Werner.Herr/DYNBET>
- [5] R. Tomas, Private communication, (2012).

**APPENDIX A: OPTICAL FUNCTIONS
DURING A SCAN**

σ	β_x	β_y			
0.0000	0.9929	0.9915	5.1000	1.0008	0.9995
0.1000	0.9929	0.9915	5.2000	1.0008	0.9995
0.2000	0.9931	0.9915	5.3000	1.0007	0.9995
0.3000	0.9933	0.9916	5.4000	1.0007	0.9996
0.4000	0.9937	0.9918	5.5000	1.0007	0.9996
0.5000	0.9941	0.9920	5.6000	1.0007	0.9996
0.6000	0.9946	0.9922	5.7000	1.0007	0.9996
0.7000	0.9952	0.9924	5.8000	1.0007	0.9996
0.8000	0.9958	0.9927	5.9000	1.0006	0.9997
0.9000	0.9964	0.9930	6.0000	1.0006	0.9997
1.0000	0.9970	0.9933	6.1000	1.0006	0.9997
1.1000	0.9976	0.9936	6.2000	1.0006	0.9997
1.2000	0.9982	0.9939	6.3000	1.0006	0.9997
1.3000	0.9988	0.9942	6.4000	1.0006	0.9997
1.4000	0.9993	0.9946	6.5000	1.0006	0.9998
1.5000	0.9998	0.9949	6.6000	1.0005	0.9998
1.6000	1.0003	0.9952	6.7000	1.0005	0.9998
1.7000	1.0006	0.9955	6.8000	1.0005	0.9998
1.8000	1.0010	0.9958	6.9000	1.0005	0.9998
1.9000	1.0012	0.9961	7.0000	1.0005	0.9998
2.0000	1.0014	0.9963	7.1000	1.0005	0.9998
2.1000	1.0016	0.9966	7.2000	1.0005	0.9998
2.2000	1.0017	0.9968	7.3000	1.0005	0.9998
2.3000	1.0018	0.9971	7.4000	1.0005	0.9999
2.4000	1.0019	0.9973	7.5000	1.0005	0.9999
2.5000	1.0019	0.9974	7.6000	1.0005	0.9999
2.6000	1.0019	0.9976	7.7000	1.0005	0.9999
2.7000	1.0018	0.9978	7.8000	1.0005	0.9999
2.8000	1.0018	0.9979	7.9000	1.0004	0.9999
2.9000	1.0018	0.9981	8.0000	1.0004	0.9999
3.0000	1.0017	0.9982			
3.1000	1.0017	0.9983			
3.2000	1.0016	0.9984			
3.3000	1.0015	0.9985			
3.4000	1.0015	0.9986			
3.5000	1.0014	0.9987			
3.6000	1.0014	0.9988			
3.7000	1.0013	0.9989			
3.8000	1.0012	0.9989			
3.9000	1.0012	0.9990			
4.0000	1.0011	0.9991			
4.1000	1.0011	0.9991			
4.2000	1.0011	0.9992			
4.3000	1.0010	0.9992			
4.4000	1.0010	0.9993			
4.5000	1.0010	0.9993			
4.6000	1.0009	0.9993			
4.7000	1.0009	0.9994			
4.8000	1.0009	0.9994			
4.9000	1.0008	0.9994			
5.0000	1.0008	0.9995			